Peptide Modulators

Deutsche Ausgabe: DOI: 10.1002/ange.201602806
Internationale Ausgabe: DOI: 10.1002/anie.201602806

An In-tether Chiral Center Modulates the Helicity, Cell Permeability, and Target Binding Affinity of a Peptide

Kuan Hu, Hao Geng, Qingzhou Zhang, Qisong Liu, Mingsheng Xie, Chengjie Sun, Wenjun Li, Huacan Lin, Fan Jiang, Tao Wang, Yun-Dong Wu,* and Zigang Li**

Abstract: *The addition of a precisely positioned chiral center in the tether of a constrained peptide is reported, yielding two separable peptide diastereomers with significantly different helicity, as supported by circular dichroism (CD) and NMR spectroscopy. Single crystal X-ray diffraction analysis suggests that the absolute configuration of the in-tether chiral center in helical form is R, which is in agreement with theoretical simulations. The relationship between the secondary structure of the short peptides and their biochemical/biophysical properties remains elusive, largely because of the lack of proper controls. The present strategy provides the only method for investigating the influence of solely conformational differences upon the biochemical/biophysical properties of peptides. The significant differences in permeability and target binding affinity between the peptide diastereomers demonstrate the importance of helical conformation.*

The majority of protein–protein interactions (PPIs) involve α-helices and are generally considered to be undruggable with small molecules because of their large interaction areas and shallow surfaces.[1] Therefore, continuous efforts are invested in developing constrained peptides for modulating PPIs by enhancing the helicity of short peptides[2–19] and peptidomimetics.[20] Numerous strategies have been investigated in this area, which generally rely on constrained peptides stabilized by aryl, alkenyl, or amide tethers.[21] The influence of a peptide's conformation on its biochemical/biophysical properties has been studied extensively.[22] However, it is difficult to examine solely conformational effects on biochemical/biophysical properties when the peptides being compared have different chemical compositions.

We wished to examine whether a chiral center in the tether of a stapled peptide, as shown in Figure 1, could influence the secondary structure and physical properties of the peptide. To this end, we synthesized a series of stabilized peptides containing a carbon atom chiral center within the tether. We have found that a precisely positioned chiral center significantly improves the α-helical contents, protease resistance, and cell permeability. We also found that the chiral center modulates target binding affinity. Meanwhile, Moore et al. have reported that a chiral center on the tether of a stapled peptide has some influences on the peptide's secondary structure.[19]

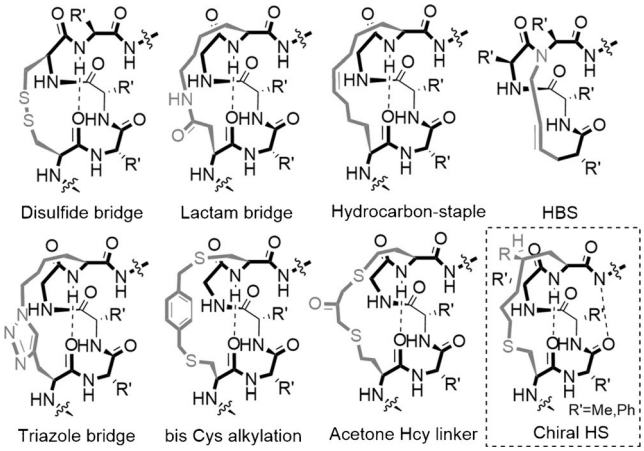

Figure 1. The α-helical peptide constrained strategies developed by others and by our group. (HBS (hydrogen bond surrogate), Hcy (homocysteine), Chiral HS (chiral hydrocarbon staple)).

To eliminate possible amino acid residue perturbations, a single turn pentapeptide system was employed as a model system, based on previous literature.[11] The structure–activity relationship of the tether ring sizes and chiral center positions are summarized in Figure S1 (Supporting Information) and the optimal tether is shown in Figure 2. Cyclic peptides **1a** and **1b** were synthesized from the linear peptide **1**, cyclo-Ac-CAAAA$_5$(2-Me)-NH$_2$ (S$_5$ ((*S*)-pentenylglycine), 2-Me (the methyl group located at the β-position with respect to the α-carbon of the amino acid)), by a thiol-ene reaction as shown in Figure 2A. Peptides **1a** and **1b** were readily separated by reverse-phase HPLC, suggesting significant conformational differences in solution. All peptides categorized in group **b** have longer retention times when compared to their diastereomers in group **a**. Circular dichroism (CD) spectroscopy measurements clearly show that peptide **1a** is a random coil, while **1b** is helical in PBS buffer (pH = 7.0; Figure 2B).

A series of single turn peptides with varying sequences were tested (peptides **2a**/**2b** to peptides **10a**/**10b**). In all cases, including glycine residue-containing peptide **8a**/**8b**, the **b** diastereomers showed enhanced helicity while the **a**

[*] K. Hu, H. Geng, Q. Zhang, Q. Liu, M. Xie, C. Sun, W. Li, H. Lin, Dr. F. Jiang, Prof. Y.-D. Wu, Prof. Z.-G. Li
School of Chemical Biology and Biotechnology
Peking University Shenzhen Graduate School
Shenzhen, 518055 (China)
E-mail: wuyd@pkusz.edu.cn
lizg@pkusz.edu.cn
Prof. T. Wang
Department of Biology
Southern University of Science and Technology
Shenzhen, 518055 (China)
E-mail: wangtao@sustc.edu.cn

Supporting information for this article can be found under: http://dx.doi.org/10.1002/anie.201602806.

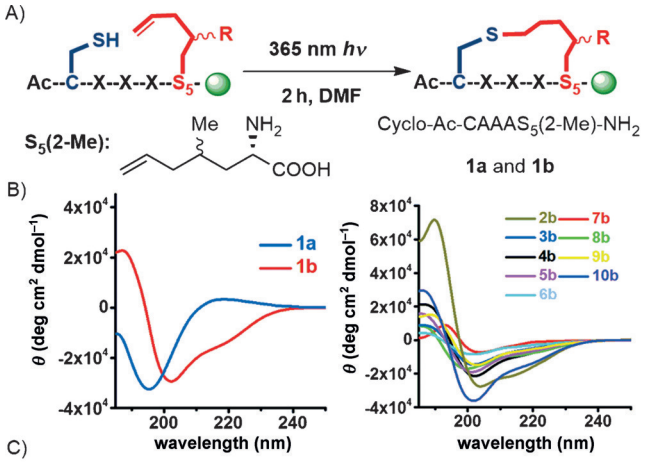

entry	peptide	$[\theta]_{222}$	$[\theta]_{205}$	$[\theta]_{190}$	Helicity*
1b	cyclo-CAAAS$_5$(2-Me)	-11792	-27010	17974	0.87
2b	cyclo-CAAAS$_5$(2-Ph)	-13780	-27001	70588	1
3b	cyclo-CAIAS$_5$(2-Me)	-4415	-13138	6425	0.37
4b	cyclo-CAEAS$_5$(2-Me)	-6784	-19340	17519	0.53
5b	cyclo-CASAS$_5$(2-Me)	-5761	-16485	9514	0.46
6b	cyclo-CAQAS$_5$(2-Me)	-2682	-7651	2403	0.26
7b	cyclo-CAFAS$_5$(2-Me)	-977	-7170	5469	0.14
8b	cyclo-CAGAS$_5$(2-Me)	-6931	-14272	3080	0.54
9b	cyclo-CEAKS$_5$(2-Me)	-4751	-13750	14232	0.4
10b	cyclo-CAAIS$_5$(2-Me)	-12139	-32516	23162	0.9

Figure 2. Helicity enhancements with an in-tether chiral center. A) Constrained peptide preparation. Optimization of tether ring size and chiral center positions are summarized in Figure S1 (Supporting Information). B) CD spectra of cyclic pentapeptides **1a**/**1b** and **2b**–**10b** in PBS (pH = 7.0) at 20 °C. C) Molar ellipticities and percentage of helicity of peptides **1b**–**10b** in PBS (pH = 7.0) at 20 °C. *The α-helical content of each peptide was calculated as reported previously. The final helical content presented relative to peptide **2b**, where the helicity of peptide **2b** is fixed at 100 %.[11]

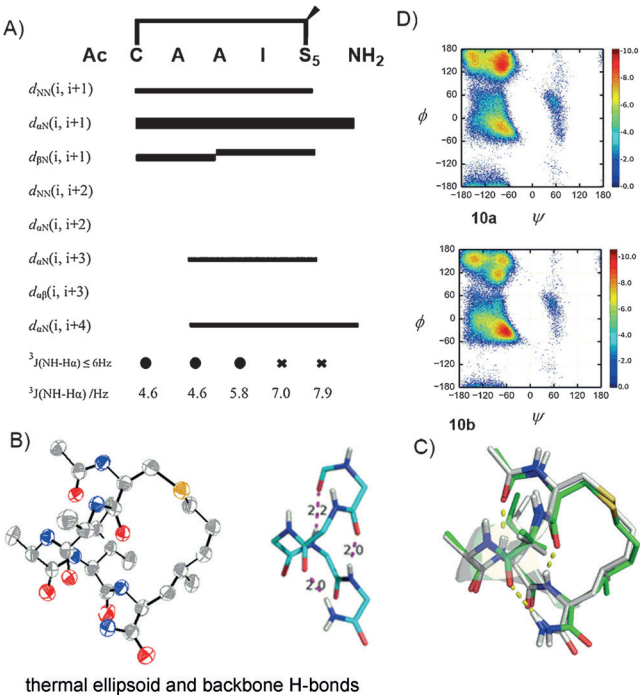

Figure 3. Conformation analysis of peptide **10a**/**10b** cyclo-Ac-CAA IS$_5$(2-Me)-NH$_2$. A) NOE summary diagram of **10b** (measured in 10 % D$_2$O in H$_2$O, 25 °C). Bar thickness reveals the intensity of the NOE signals. B) Thermal ellipsoid and backbone H-bonds in a crystal structures of pentapeptide **10b** cyclo-Ac-CAAIS$_5$(2-Me)-NH$_2$. C) Calculated structure of peptide **10b** superimposed with the solved structure. Each simulation was performed over 200 ns for sufficient sampling. Snapshots used for analysis were taken at room temperature (300 K) and conformational clustering conducted using a backbone dihedral-based method. D) Ramachandran plots of **10a/b** from an REMD simulation; upper **10a**, lower **10b**.

diastereomers were mainly random coils. These results are summarized in Figure 2B (see Supporting Information, Figure S2 for CD spectra of diastereomers **2a**–**10a**). Additionally, peptide **1b** remains helical at high temperature and at high concentrations of guanidinium hydrochloride (Supporting Information, Figure S3).

Detailed 1D and 2D ^{1}H-NMR spectroscopic studies of **1b, 2b**, and **10b** were performed in 10 % D$_2$O in H$_2$O at 25 °C. As expected, a number of spectral features were observed that are characteristic of the well-defined structure in the cyclic pentapeptides, and are specifically characteristic of α-helicity (except the C terminal residue S$_5$(2-Me/2-Ph)). Firstly, conspicuously low coupling constants were observed ($^3J_{\text{NH-Cha}} <$ 6 Hz) for all amide resonances except S5(2-Me/2-Ph) (Figure 3A; Supporting Information, Figure S4A), as normally observed in α-helical peptides.[22] Secondly, the observation in NOESY spectra of nonsequential medium range $d\alpha N(i, i+3)$, $d\alpha\beta(i, i+3)$, and $d\alpha N(i, i+4)$ NOEs suggest a helical structure (Figure 3A; Supporting Information, Figure S4B). Furthermore, the temperature coefficients of the backbone amide NH chemical shifts of **1b** were determined, with temperature coefficients ($\Delta\delta/T$) less than 4 ppb K$^-$ for C5 and A2 (Supporting Information, Figure S4C), consistent with their involvement in hydrogen bonding typical of an α- or 3_{10}-helix. In summary, the NOE and CD spectra of peptides **1b**, **2b**, and **10b** suggest that they adopt a mixture of 3_{10}- and α-helical conformations in solution.

As shown in Figure 3B, X-ray diffraction analysis of peptide **10b** cyclo-Ac-CAAIS$_5$(2-Me)-NH$_2$ unambiguously confirms that the absolute configuration of the in-tether chiral center is *R*. The backbone dihedral angle set is summarized in Table SI (Supporting Information), and all dihedral angle values are close to that of a standard α-helix (except for the C terminal residue). Additionally, the methyl group at the chiral center protrudes from the peptide backbone. Therefore, a chiral center in the tether provides a modifiable site that can lead to more effective peptide ligands or serve to improve the drug-like properties of the peptide.

To improve our understanding of the conformational features of different peptide diastereomers, we performed replica exchange molecular dynamics (REMD) simulations with explicit water using the recently developed force field RSFF2. For peptide **10b**, the most distributed structure derived from the simulation is almost identical to the solved structure (backbone + Cβ rmsd: 0.3 Å) as shown in Figure 3C. The Ramachandran plots (ϕ,ψ distribution) of

the two diastereomers in the simulations, exhibit different conformational preferences (Figure 3D; Supporting Information). For the S-diastereomer **10a**, the dominant calculated structures are shown in Figures S5 and S6 (Supporting Information), and demonstrate no significant secondary structures, which is in excellent agreement with the CD results. Further simulation of a peptide without the in-tether R-substitution group (Ac-cyclo-CAAAS$_5$(2-H)-NH$_2$) indicates that the polyproline-II (PII) conformation is intrinsically favored by the residues, and the representative structure of the most populated cluster is not helical (Supporting Information, Figure S5A). In this non-helical structure, an R = CH$_3$/Ph substitution with (*S*)-chirality can be added without any steric interference (Supporting Information, Figure S5B). However, the non-helical structure is significantly destabilized when an R = CH$_3$ substitution group is placed in (*R*)-chirality, and is very comfortable when the peptide backbone adopts an α-helical conformation (Supporting Information, Figure S5C). A larger R = Ph group in (*R*)-chirality lead to higher destabilization of non-helical structures, and a stronger preference for an α-helical conformation (Supporting Information, Figure S5D). More detailed information can be found in Figures S6–S8 (Supporting Information).

The influence of conformation on the biochemical/biophysical properties of peptides remains unclear, largely because of the absence of methods for constructing peptides with minimal differences in chemical composition. Cell permeability is the major limitation for peptide therapeutics and is influenced by many aspects, including conformation.[23] Scrambling the positions of a few amino acids in a peptide can dramatically change permeability and other biophysical properties. To date, our strategy provides the only method for specifically investigating the sole influence of conformational differences. Firstly, peptide diastereomers **11a/11b** FITC-βA-[cyclo-CRARS$_5$(2-Ph)]-NH$_2$ and **12a/12b** FITC-βA-[cyclo-CRRRS$_5$(2-Ph)]-NH$_2$ (βA (beta alanine), FITC (fluorescein isothiocyanate)) were synthesized and separated. As shown in Figure 4, the helical diastereomers **11b** and **12b** could successfully penetrate HEK293T cells within 2 h while the other diastereomers were much less permeable (Figure 4A). This led us to consider whether a helical conformation itself could make peptides permeable. Peptide diastereomers **13a/13b** FITC-βA-[cyclo-CAKAS$_5$(2-Ph)]-NH$_2$ were subsequently tested. Peptide **13b** showed enhanced helicity over peptide **13a** (Supporting Information, Figure S9A). However, while peptide **13b** outperformed peptide **13a** in terms of penetration of the cell membrane, it only showed minimal penetrative efficacy (Supporting Information, Figures S9B and S9C). These results suggest that, although helical conformation itself may not guarantee the permeability of peptides, it is a determining factor. The structural elucidation of estrogen receptor alpha (ERα) and mammal double minute 2 (MDM2) with their constrained peptide ligands clearly showed the interaction between the protein targets and the ligand tethers, mostly in the flat hydrophobic region surrounding the target ligand binding site.[24] Based on the results, we chose these two model targets to study the influence of peptide helicity and

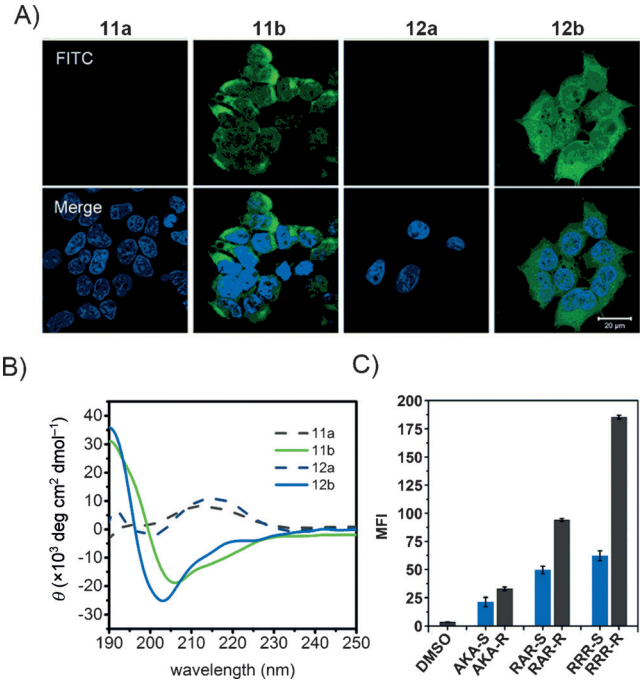

Figure 4. Cell permeability of pentapeptide diastereomers. A) Fluorescent confocal microscopy images of HEK293T cells incubated with FITC labeled peptides **11a/b** and **12a/b** (5 μM) at 37°C for 2 h (blue (DAPI), green (FITC)). B) CD spectra of peptides **11a/b** and **12a/b** at 20°C in 50% TFE buffer. C) Flow cytometry measurements of HEK293T cells with peptide **11a/b**, **12a/b**, and **13a/b** (5 μM) at 37°C for 2 h.

substitution groups at the tether chiral center on the target binding affinity of the peptide. **ER-1 a/b** and **ER-2 a/b** were synthesized based on their reported sequences (Figure 5A),[24a] which contain a methyl or phenyl group at the chiral center, respectively. **ER-1b** and **ER-2b** showed a significant increase in helicity compared to **ER-1a** and **ER-2a** (Figure 5B). The binding affinity of **ER-1b** (ca. 1 nM) and **ER-2b** (ca. 69 nM) is much better than that for **ER-1a** (ND) and **ER-2a** (> 600 nm; Figure 5C,D). Interestingly, **ER-1b** showed a significantly enhanced binding affinity compared to all previously reported ER-α peptide ligands, which may be caused by the additional interaction contributed by the methyl group at the stereocenter in the tether with the ERα protein. Peptides **PDI-1a/b** and **PDI-2a/b** were also synthesized based on their reported sequences.[25] **PDI-1b** and **2b** showed a remarkable increase in helicity compared to **PDI-1a** and **2a** (Figure 5E). They also showed significantly better binding affinities than **PDI-1a** and **2a** (Figure 5F,G). However, **PDI-2b** showed unfavorable binding (ca. 504 nM) compared to **PDI-1b** (ca. 165 nM), which may be caused by the steric hindrance imposed by the bulky phenyl group and MDM2. These results constitute the first direct evidence of a direct relationship between helical enhancement and peptide ligand/protein target binding. Moreover, these results suggest that the substitution group also interacts directly with the binding groove, providing a valuable modification site for future applications, such as fragment-based peptide ligand design.

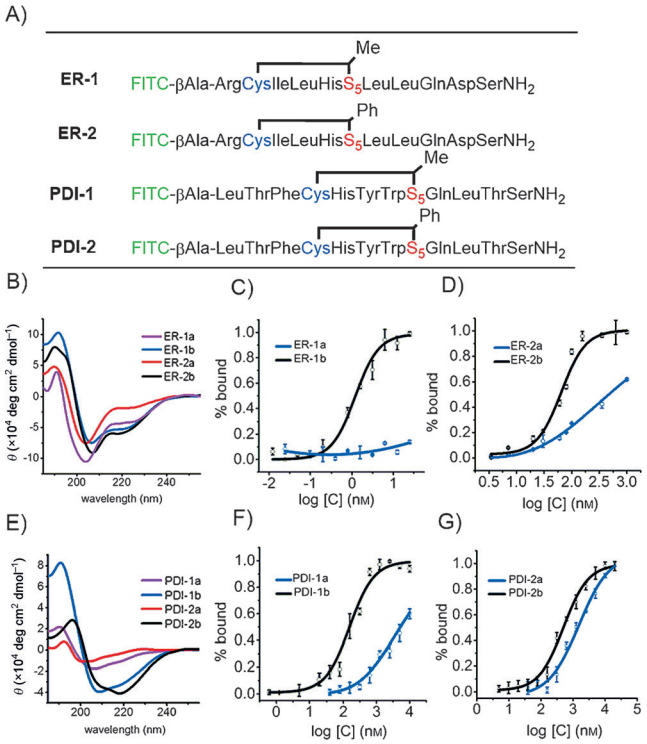

Figure 5. Target binding affinity of **ERα** and **MDM2** with their peptide ligand diastereomers. A) Representation of **ER-1a/1b**, **ER-2a/2b**, **PDI-1a/1b**, and **PDI-2a/2b** structures. B) CD spectra of ER peptides, measured in 20% TFE buffer solution at 20°C. C and D) Binding of **ER-1a/1b** and **ER-2a/2b** with ERα, respectively. The binding affinities were measured using fluorescence polarization assays (FP) at 20°C. E) CD spectra of PDI peptides, measured in 20% TFE buffer solution at 20°C. F and G) Binding of **PDI-1a/1b** and **PDI-2a/2b** with MDM2, respectively. The binding affinities were measured using fluorescence polarization assays (FP) at 20°C.

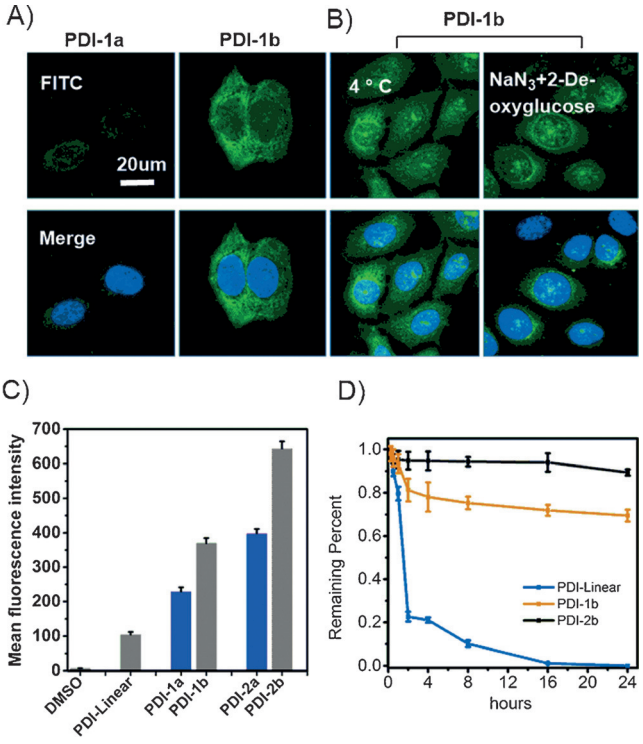

Figure 6. Cell permeability and in vitro serum stability of PDI peptides. A) Fluorescent confocal microscopy images of MCF-7 cells incubated with FITC labeled peptides **PDI-1a/1b** (5 μM) at 37°C. B) Fluorescent confocal microscopy images of MCF-7 cells incubated with FITC labeled peptides **PDI-1b** (5 μM) at 4°C or treated with NaN_3 and 2-deoxyglucose for 1 h (DNA, blue (DAPI) peptides, green (FITC)). C) FACS measurements of MCF-7 cells treated with **ER-1a/1b**, **PDI-1a/1b**, and **PDI-2a/2b** (5 μM) at 37°C. For separated flow cytometry figures, see Figure S10 (Supporting Information). D) In vitro serum digestion assay of **PDI-linear**, **PDI-1b**, and **PDI-2b** peptides.

Notably, cellular uptake experiments using MCF-7 cells treated with 5 μM peptides (**ER-1a/1b**, **PDI-1a/1b**) revealed that **PDI-1b** and **ER-1b** show significantly higher uptakes than their diastereomers (Figure 6A; Supporting Information, Figure S10). These results were further confirmed by flow cytometry measurement (Figure 6C; Supporting Information, Figures S10B–D). The peptide continued to penetrate the cell membrane when incubated at 4°C or with the addition of sodium azide (Figure 6B). This observation suggests that the permeability mechanism partly involves transduction, which could be explained by the hydrophobic tether. The latter is produced by the hydrophobic substitution group as well as cyclization. The in vitro serum stability assay showed that the **PDI-Linear** peptide degraded in a few hours, while more than 70% of peptides **PDI-1b** and **PDI-2b** remained intact after 24 hours (Figure 6D). Notably, the bulkier substitution group showed better proteolysis resistance. Thus, chiral center-induced helicity enhancement was successfully translated into longer peptides with good binding affinity and intriguing cell permeability.

In summary, a precisely positioned in-tether carbon chiral center was capable of modulating the helicity of a peptide. This study provides an excellent means for evaluating the relationship between conformation and biochemical/biophysical properties of peptides. We investigated the relationship between the helicities of the peptides and the location of the chiral center, the stereoconfiguration, the ring size, and the size of the substitution group. The pentapeptide crystal structure and computational simulations further validate our results. Peptide diastereomers were also tested to examine the sole influence of conformation on cell permeability.

Moreover, this concept was applied to construction of MDM2 and ERα peptide ligands, which show excellent α-helicity nucleation properties and dramatically enhanced binding affinities. More importantly, the significant differences in the permeability of the long peptide diastereomers clearly indicate the importance of increasing peptide helicity in the construction of constrained peptides. Furthermore, the influence of the substitution groups at the chiral center on the binding affinity of peptides suggests that this chiral center could be utilized as an additional modification site away from the peptide backbone. Consequently, this feature may be useful for various applications. Studies on the effect of the chiral center and the implications for biological applications are currently underway and will be reported in due time.

Acknowledgements

This work is supported by the National Natural Science Foundation of China (Grant 21102007 (Z.L.), 31300600 (T.W.), and 21372023 (Z.L.)), MOST 2015DFA31590 (Z.L.), MOST 2013CB911500 (T.W.). The Shenzhen Science and Technology Innovation Committee (SW201110018, SGLH20120928095602764, ZDSY20130331145112855, KQCX20130627, and JSGG20140519105550503 (Z.L.) KQCX20130627103353535 (T.W.)), and the Shenzhen Peacock Program (KQTD201103 (Z.L.)).

Keywords: cell permeability · chirality · helicity · stapled peptide · target binding affinity

How to cite: *Angew. Chem. Int. Ed.* **2016**, *55*, 8013 – 8017
Angew. Chem. **2016**, *128*, 8145 – 8149

[1] a) H. Yin, A. D. Hamilton, *Angew. Chem. Int. Ed.* **2005**, *44*, 4130 – 4163; *Angew. Chem.* **2005**, *117*, 4200 – 4235; b) V. Azzarito, K. Long, N. S. Murphy, A. J. Wilson, *Nat. Chem.* **2013**, *5*, 161 – 173; c) L.-G. Milroy, T. N. Grossmann, S. Hennig, L. Brunsveld, C. Ottmann, *Chem. Rev.* **2014**, *114*, 4695 – 4748.
[2] G. Osapay, J. W. Taylor, *J. Am. Chem. Soc.* **1990**, *112*, 6046 – 6051.
[3] J. C. Phelan, N. J. Skelton, A. C. Braisted, R. S. McDowell, *J. Am. Chem. Soc.* **1997**, *119*, 455 – 460.
[4] J. H. B. Pease, R. W. Storrs, D. E. Wemmer, *Proc. Natl. Acad. Sci. USA* **1990**, *87*, 5643 – 5647.
[5] D. Y. Jackson, D. S. King, J. Chmielewski, S. Singh, P. G. Schultz, *J. Am. Chem. Soc.* **1991**, *113*, 9391 – 9392.
[6] E. Cabezas, A. C. Satterthwait, *J. Am. Chem. Soc.* **1999**, *121*, 3862 – 3875.
[7] J. R. Kumita, O. S. Smart, G. A. Woolley, *Proc. Natl. Acad. Sci. USA* **2000**, *97*, 3803 – 3808.
[8] C. E. Schafmeister, J. Po, G. L. Verdine, *J. Am. Chem. Soc.* **2000**, *122*, 5891 – 5892.
[9] A. M. Leduc, J. O. Trent, J. L. Wittliff, K. S. Bramlett, S. L. Briggs, N. Y. Chirgadze, Y. Wang, T. P. Burris, A. F. Spatola, *Proc. Natl. Acad. Sci. USA* **2003**, *100*, 11273 – 11278.
[10] A. K. Galande, K. S. Bramlett, T. P. Burris, J. L. Wittliff, A. F. Spatola, *J. Pept. Res.* **2004**, *63*, 297 – 302.
[11] N. E. Shepherd, H. N. Hoang, G. Abbenante, D. P. Fairlie, *J. Am. Chem. Soc.* **2005**, *127*, 2974 – 2983.
[12] S. Cantel, A. Le Chevalier Isaad, M. Scrima, J. J. Levy, R. D. DiMarchi, P. Rovero, J. A. Halperin, A. M. D'Ursi, A. M. Papini, M. Chorev, *J. Org. Chem.* **2008**, *73*, 5663 – 5674.
[13] A. Muppidi, K. Doi, S. Edwardraja, E. J. Drake, A. M. Gulick, H. G. Wang, Q. Lin, *J. Am. Chem. Soc.* **2012**, *134*, 14734 – 14737.
[14] Y. H. Lau, P. de Andrade, S.-T. Quah, M. Rossmann, L. Laraia, N. Skold, T. J. Sum, P. J. E. Rowling, T. L. Joseph, C. Verma, M. Hyvonen, L. S. Itzhaki, A. R. Venkitaraman, C. J. Brown, D. P. Lane, D. R. Spring, *Chem. Sci.* **2014**, *5*, 1804 – 1809.
[15] C. M. Haney, W. S. Horne, *J. Pept. Sci.* **2014**, *20*, 108 – 114.
[16] Y. Zou, A. M. Spokoyny, C. Zhang, M. D. Simon, H. Yu, Y.-S. Lin, B. L. Pentelute, *Org. Biomol. Chem.* **2014**, *12*, 566 – 573.
[17] G. J. Hilinski, Y.-W. Kim, J. Hong, P. S. Kutchukian, C. M. Crenshaw, S. S. Berkovitch, A. Chang, S. Ham, G. L. Verdine, *J. Am. Chem. Soc.* **2014**, *136*, 12314 – 12322.
[18] D. Mazzier, C. Peggion, C. Toniolo, A. Moretto, *Biopolymers* **2014**, *102*, 115 – 123.
[19] T. E. Speltz, S. W. Fanning, C. G. Mayne, C. Fowler, E. Tajkhorshid, G. L. Greene, T. W. Moore, *Angew. Chem. Int. Ed.* **2016**, *55*, 4252 – 4255; *Angew. Chem.* **2016**, *128*, 4324 – 4327.
[20] a) A. Kritzer, J. D. Lear, M. E. Hodsdon, A. Schepartz, *J. Am. Chem. Soc.* **2004**, *126*, 9468 – 9469; b) A. Kritzer, O. M. Stephens, D. A. Guarracino, S. K. Reznik, A. Schepartz, *Bioorg. Med. Chem.* **2005**, *13*, 11 – 16; c) D. Sadowsky, M. A. Schmitt, H.-S. Lee, N. Umezawa, S. Wang, Y. Tomita, S. H. Gellman, *J. Am. Chem. Soc.* **2005**, *127*, 11966 – 11968; d) D. Seebach, J. Gardiner, *Acc. Chem. Res.* **2008**, *41*, 1366 – 1375; e) S. Horne, L. M. Johnson, T. J. Ketas, P. J. Klasse, M. Lu, J. P. Moore, S. H. Gellman, *Proc. Natl. Acad. Sci. USA* **2009**, *106*, 14751 – 14756; f) M. Johnson, S. H. Gellman, *Methods Enzymol.* **2013**, *523*, 407 – 429.
[21] a) L. K. Henchey, A. L. Jochim, P. S. Arora, *Curr. Opin. Chem. Biol.* **2008**, *12*, 692 – 697; b) T. A. Hill, N. E. Shepherd, F. Diness, D. P. Fairlie, *Angew. Chem. Int. Ed.* **2014**, *53*, 13020 – 13041; *Angew. Chem.* **2014**, *126*, 13234 – 13257; c) L. D. Walensky, G. H. Bird, *J. Med. Chem.* **2014**, *57*, 6275 – 6288; d) Y. H. Lau, P. de Andrade, Y. Wu, D. R. Spring, *Chem. Soc. Rev.* **2015**, *44*, 91 – 102.
[22] K. Wüthrich, M. Billeter, W. Braun, *J. Mol. Biol.* **1984**, *180*, 741 – 751.
[23] a) T. Rezai, J. E. Bock, M. V. Zhou, C. Kalyanaraman, R. S. Lokey, M. P. Jacobson, *J. Am. Chem. Soc.* **2006**, *128*, 14073 – 14080; b) T. Rezai, B. Yu, G. L. Millhauser, M. P. Jacobson, R. S. Lokey, *J. Am. Chem. Soc.* **2006**, *128*, 2510 – 2511; c) Q. Chu, R. E. Moellering, G. J. Hilinski, Y.-W. Kim, T. N. Grossmann, J. T. H. Yeh, G. L. Verdine, *MedChemComm* **2015**, *6*, 111 – 119; d) V. Boguslavsky, V. J. Hruby, D. F. O'Brien, A. Misicka, A. W. Lipkowski, *J. Pept. Res.* **2003**, *61*, 287 – 297.
[24] a) C. Phillips, L. R. Roberts, M. Schade, R. Bazin, A. Bent, N. L. Davies, R. Moore, A. D. Pannifer, A. R. Pickford, S. H. Prior, C. M. Read, A. Scott, D. G. Brown, B. Xu, S. L. Irving, *J. Am. Chem. Soc.* **2011**, *133*, 9696 – 9699; b) S. Baek, P. S. Kutchukian, G. L. Verdine, R. Huber, T. A. Holak, K. W. Lee, G. M. Popowicz, *J. Am. Chem. Soc.* **2012**, *134*, 103 – 106; c) Y. S. Chang, B. Graves, V. Guerlavais, C. Tovar, K. Packman, K.-H. To, K. A. Olson, K. Kesavan, P. Gangurde, A. Mukherjee, T. Baker, K. Darlak, C. Elkin, Z. Filipovic, F. Z. Qureshi, H. Cai, P. Berry, E. Feyfant, X. E. Shi, J. Horstick, D. A. Annis, A. M. Manning, N. Fotouhi, H. Nash, L. T. Vassilev, T. K. Sawyer, *Proc. Natl. Acad. Sci. USA* **2013**, *110*, E3445 – E3454.
[25] B. Hu, D. M. Gilkes, J. Chen, *Cancer Res.* **2007**, *67*, 8810 – 8817.

Received: March 21, 2016
Published online: May 11, 2016

